MOLECULAR AND CELLULAR BIOLOGY, Oct. 2002, p. 7184–7192 Vol. 22, No. 20
0270-7306/02/$04.00+0 DOI: 10.1128/MCB.22.20.7184–7192.2002


# Structural Basis for Activation of Fibroblast Growth Factor Signaling by Sucrose Octasulfate

Brian K. Yeh,[1] Anna V. Eliseenkova,[1] Alexander N. Plotnikov,[1]† David Green,[2] Jared Pinnell,[2] Tulay Polat,[3] Amel Gritli-Linde,[4] Robert J. Linhardt,[3] and Moosa Mohammadi[1]*

*Departments of Pharmacology[1] and Medicine,[2] New York University School of Medicine, New York, New York 10016; Departments of Chemistry, Medicinal and Natural Products Chemistry, and Chemical and Biochemical Engineering, University of Iowa, Iowa City, Iowa 52242[3]; and Department of Oral Biochemistry, Göteborg University, Göteborg, Sweden[4]*

Received 9 May 2002/Returned for modification 9 July 2002/Accepted 19 July 2002

**Sucrose octasulfate (SOS) is believed to stimulate fibroblast growth factor (FGF) signaling by binding and stabilizing FGFs. In this report, we show that SOS induces FGF-dependent dimerization of FGF receptors (FGFRs). The crystal structure of the dimeric FGF2-FGFR1-SOS complex at 2.6-Å resolution reveals a symmetric assemblage of two 1:1:1 FGF2-FGFR1-SOS ternary complexes. Within each ternary complex SOS binds to FGF and FGFR and thereby increases FGF-FGFR affinity. SOS also interacts with the adjoining FGFR and thereby promotes protein-protein interactions that stabilize dimerization. This structural finding is supported by the inability of selectively desulfated SOS molecules to promote receptor dimerization. Thus, we propose that SOS potentiates FGF signaling by imitating the dual role of heparin in increasing FGF-FGFR affinity and promoting receptor dimerization. Hence, the dimeric FGF-FGFR-SOS structure substantiates the recently proposed "two-end" model, by which heparin induces FGF-FGFR dimerization. Moreover, the FGF-FGFR-SOS structure provides an attractive template for the development of easily synthesized SOS-related heparin agonists and antagonists that may hold therapeutic potential.**

Fibroblast growth factors (FGFs; FGF1 to FGF22) regulate a wide array of physiological processes including embryogenesis, cell growth, differentiation, angiogenesis, tissue repair, and wound healing (30). The diverse activities of FGFs are mediated by four receptor tyrosine kinases (FGFR1 to FGFR4), each composed of an extracellular ligand-binding portion consisting of three immunoglobulin-like domains (D1 to D3), a single transmembrane helix, and a cytoplasmic portion with protein tyrosine kinase activity (18).

Receptor dimerization is an obligatory event in FGF signaling and requires heparin or heparan sulfate proteoglycans (28). Two contrasting mechanisms for FGF receptor (FGFR) dimerization have emerged from the recent crystal structures of FGF-FGFR-heparin complexes. In the "two-end" model, deduced from the FGF2-FGFR1-heparin crystal structure, two 1:1:1 FGF-FGFR-heparin ternary complexes form a symmetric dimer (40). Each FGF binds to both receptors, and there is a direct contact between the two FGFRs. Within each ternary complex, heparin interacts extensively with FGF and FGFR, thereby enhancing FGF-FGFR affinity. Heparin also binds to the FGFR across the twofold dimer and thereby fortifies the interactions of FGF and FGFR from one ternary complex with FGFR in the other ternary complex. Thus, heparin fulfils an adapter role in receptor dimerization.

In the model derived from the FGF1-FGFR2-heparin structure (33), a single heparin oligosaccharide bridges two FGF molecules into a dimer that in turn brings two receptor chains together. Heparin makes a different set of contacts with the two ligands and binds to one receptor only, resulting in the distinctive asymmetry of the dimer. Unlike the configuration in the two-end model, each FGF contacts a single FGFR and there is no direct FGFR-FGFR contact. The total lack of protein-protein interface between the two FGF-FGFR monomers in the dimer means that heparin is absolutely necessary for receptor dimerization in this model.

Besides heparin, a number of chemically diverse low-molecular-weight sulfated sugars such as sucrose octasulfate (SOS) have been reported to potentiate FGF action. SOS has been shown to mimic heparin action in supporting FGF-induced neoangiogenesis and cell proliferation in vitro (2, 11, 23, 29, 45, 49). Moreover, SOS facilitates wound healing by enhancing FGF-induced angiogenesis (39). The molecular mechanism by which SOS stimulates FGF signaling is not fully understood. Since SOS binds and protects FGFs against high temperature and low pH (1, 11, 45), it has been suggested that SOS enhances FGF signaling by prolonging the half-life of FGF.

However, because receptor dimerization is mandatory for activation of FGF signaling, we reasoned that the heparin-like activity of SOS must involve FGFR dimerization as well. In this report, we first confirm the heparin-like activity of SOS in an FGF-dependent-differentiation assay. Next, we demonstrate that SOS induces FGF-FGFR dimerization in vitro. Finally, we determine the crystal structure of the dimeric FGF-FGFR-SOS complex. Analysis of this dimeric structure reveals that SOS induces FGF-FGFR dimerization with a mode and stoichiometry reminiscent of the two-end model. Thus, we con-

* Corresponding author. Mailing address: Department of Pharmacology, New York University School of Medicine, New York, NY 10016. Phone: (212) 263-2907. Fax: (212) 263-7133. E-mail: mohammad@saturn.med.nyu.edu.

† Present address: Plexxikon Inc., Berkeley, CA 94710.

clude that SOS stimulates FGF signaling by imitating heparin in increasing FGF-FGFR affinity and promoting dimerization. Our structural finding gives strong credence to the two-end dimerization model.

## MATERIALS AND METHODS

**Organ culture and in situ hybridization.** For embryo staging, the day of evidence of a vaginal plug was considered as 0.5 day postcoitum (dpc). Calvaria were dissected from 16.5-dpc mouse embryos (NMRI strain). The dura mater was left intact in all explants. Explants were cultured for 9 days in a Trowell-type organ culture system on 0.8-μm-pore-size Costar filters supported by metal grids. The serum-free culture medium consisted of BGJb medium (Gibco) containing 0.1% bovine serum albumin, 40 μg of transferrin/ml, 2 mM Glutamax, 150 μg of ascorbic acid/ml, and antibiotics (14). The explants (four or five specimens per group) were cultured in the absence or presence of FGF2 (50 ng/ml), heparin (10 μM; molecular weight, 3,000; Sigma), or SOS (50 or 200 μM), alone or in combination.

After 9 days of culture, the calvaria were fixed in 4% paraformaldehyde in 0.1 M phosphate buffer, pH 7.4, and processed for paraffin embedding. Six-micrometer serial sections were prepared for hybridization with a $^{35}$S-UTP-labeled riboprobe as previously described (46). An *Eco*RI-linearized 0.35-kb osteocalcin template was transcribed with T7 RNA polymerase and used as the probe.

**Dimerization of FGF-FGFR complexes by SOS in vitro.** The ligand binding portion of FGFR1 consisting of immunoglobulin-like domain 2 (D2) and D3 was produced in *Escherichia coli* and refolded in vitro as previously described (37). The refolded FGFR1 ectodomain was then mixed with FGF2, and the resulting 1:1 FGF2-FGFR1 complexes were purified to homogeneity by size exclusion chromatography as previously described (37). The purified 1:1 FGF2-FGFR1 complexes were mixed at various molar ratios with SOS or selectively desulfated SOS analogs, and the mixtures were analyzed on a Superdex 200 size exclusion column in a 25 mM HEPES-NaOH buffer (pH 7.5) containing 150 mM NaCl.

**Crystallization and structure determination.** Dimeric 2:2:2 FGF2-FGFR1-SOS complexes were generated by mixing purified 1:1 FGF2-FGFR1 complexes with SOS at a molar ratio of 1:1. Crystals were grown by vapor diffusion at 20°C by the hanging-drop method. Two microliters of protein solution (10 mg/ml in 25 mM HEPES-NaOH [pH 7.5], 150 mM NaCl) was mixed with an equal volume of crystallization buffer (12 to 16% polyethylene glycol 5000, 0.2 M ammonium sulfate, and 15% glycerol in 0.1 M HEPES-NaOH [pH 7.5]). The FGF2-FGFR1-SOS crystals belong to orthorhombic space group $P2_12_12_1$ with a solvent content of 56% and the following unit cell dimensions: $a$ = 64.2 Å, $b$ = 122.4 Å, and $c$ = 219.5 Å. Diffraction data were collected from a flash-frozen crystal on a charge-coupled device detector at beamline X4A at the National Synchrotron Light Source, Brookhaven National Laboratory. The data were processed with DENZO and SCALEPACK (32). A molecular replacement solution was found for the four copies of the FGF2-FGFR1 complex in the asymmetric unit with the program AmoRe (26) and the FGF2-FGFR1 structure (PDB identification code, 1CVS) (37) as the search model. The initial model for SOS was taken from the FGF1-SOS crystal structure (PDB identification code, 1AFC) (50). The parameters for the SOS molecule were generated by using the HIC-Up server (22). Simulated annealing, positional, and temperature factor refinements were performed with the crystallography and NMR system (6). Bulk solvent and anisotropic B-factor corrections were applied. Tight noncrystallographic symmetry restraints were imposed throughout the refinement for the backbone atoms of FGF2, D2, and D3. Model building into the $2F_o$-$F_c$ and $F_o$-$F_c$ electron density maps was performed with program O (19). The refined model consists of 4 FGF2 molecules (residues 16 to 144), 4 FGFR1 molecules (residues 149 to 359), 4 SOS molecules, 3 sulfate ions, and 42 water molecules.

**Chemical synthesis of desulfated SOS analogs. (i) Synthesis of 1′,3′,4′,6′-tetra-*O*-sulfo-β-D-fructofuranosyl-3,4,6-tri-*O*-sulfo-α-D-glucopyranoside, heptasodium salt (2-hydroxysucrose hepatasulfate).** 2-*O*-Lauryl-β-D-fructofuranosyl α-D-glucopyranoside (320 mg, 0.6 mmol) (8) and the trimethylamine · $SO_3$ complex (880 mg, 6.3 mmol) were stirred under $N_2$ in 20 ml of dry dimethylformamide at 50°C for 12 h. The trimethylamine · $SO_3$ complex (880 mg) was again added, and the suspension was kept at 50°C for an additional 12 h. $CH_3OH$-$H_2O$ (1:1 [vol/vol]) was added, and the suspension was layered on a column of Sephadex LH-20 and eluted with the same solvent system. The combined product was passed through Dowex 50 ($Na^+$). After evaporation, the colorless glass was dissolved in water and lyophilized to give 1′,3′,4′,6′-tetra-*O*-sulfo-β-D-fructofuranosyl-2-*O*-lauryl-3,4,6-tri-*O*-sulfo-α-D-glucopyranoside, heptasodium salt as a white powder in 96% yield. The product was characterized by $^1$H nuclear magnetic resonance (NMR) and $^{13}$C NMR. 1′,3′,4′,6′-tetra-*O*-sulfo-β-D-fructofuranosyl-2-*O*-lauryl-3,4,6-tri-*O*-sulfo-α-D-glucopyranoside, heptasodium salt (120 mg) in 2.5 ml of 0.5 N NaOH was stirred overnight at 4°C. The reaction was quenched with 3 ml of 0.5 N HCl and extracted with $CHCl_3$ (three times with 5 ml). The aqueous layer was passed through Dowex 50 ($Na^+$), evaporated under high vacuum, redissolved in water, and lyophilized to give a white powder (2-hydroxysucrose hepatasulfate; 96% yield). The product was characterized by $^1$H NMR and $^{13}$C NMR.

**(ii) Synthesis of 1′,3′,4′,6′-tetra-*O*-sulfo-β-D-fructofuranosyl-2,3-di-*O*-sulfo-α-D-glucopyranoside, hexasodium salt (4,6-dihydroxysucrose hexasulfate).** Sulfonation of 4,6-*O*-isopropylidine (20) (as described above) afforded 1′,3′,4′,6′-tetra-*O*-sulfo-β-D-fructofuranosyl-4,6-*O*-isopropylidine-2,3-di-*O*-sulfo-α-D-glucopyranoside, hexasodium salt, which was characterized by $^1$H NMR and $^{13}$C NMR. 1′,3′,4′,6′-tetra-*O*-sulfo-β-D-fructofuranosyl-4,6-*O*-isopropylidine-2,3-di-*O*-sulfo-α-D-glucopyranoside (20 mg, 0.02 mmol) and 60% acetic acid (2 ml) were stirred under $N_2$ at 80°C for 20 min. The product was passed through Dowex 50 ($Na^+$). After evaporation, the colorless glass was dissolved in water and lyophilized to give 4,6-dihydroxysucrose hexasulfate as a white powder in 95% yield. The product was characterized by $^1$H NMR and $^{13}$C NMR.

**Coordinates.** The atomic coordinates of the FGF2-FGFR1-SOS structure will be deposited in the Protein Data Bank for immediate release upon publication.

## RESULTS

**SOS can replace heparin in promoting FGF-dependent cellular responses.** A large body of literature has documented that SOS can mimic heparin in potentiating FGF-induced cell proliferation and neoangiogenesis (2, 11, 23, 29, 45, 49).

To extend these studies, we decided to assess the heparin-like activity of SOS in yet another FGF-dependent system. Recent advances in human genetics have identified FGF signaling as an essential regulator of skeletal development (24). Activation of FGFR has been shown to promote the fusion of calvarial sutures by stimulating the differentiation of sutural mesenchyme into osteoblasts (21). Thus, we evaluated the ability of SOS to induce FGF-dependent fusion of calvarial sutures. Cultures of developing calvarial bones were treated with FGF2 and/or SOS and then analyzed by in situ hybridization for osteocalcin mRNA, a molecular marker for differentiated osteoblasts (5). In untreated cultures, the overlapping parietal and frontal bones in the coronal suture (Fig. 1a) and the osteogenic fronts of the parietal bones in the sagittal suture (Fig. 1b) were widely separated by undifferentiated osteocalcin-negative mesenchyme. Osteoblasts in the bone plates expressed basal levels of osteocalcin mRNA. Treatment with SOS (50 μM) or heparin (10 μM) alone resulted in no morphological changes relative to the untreated cultures (Fig. 1c, d, i, and j). However, in the presence of high concentrations of SOS (200 μM), the frontal and parietal bones at the coronal and sagittal sutures exhibited an increase in osteocalcin expression and the bone plates were separated by less undifferentiated sutural mesenchyme (Fig. 1e and f). Prolonged exposure to FGF2 alone produced morphological changes similar to those with 200 μM SOS alone (Fig. 1g and h). We attribute these modest effects to the presence of endogenous FGF2 and heparan sulfate proteoglycans in the organ cultures. Combination of FGF2 with heparin (10 μM) or SOS (50 μM) augmented the effects of FGF2 on sutural differentiation and osteocalcin expression (Fig. 1k to n). In both cases, nearly all of the mesenchyme between the osteogenic fronts in the sagittal sutures had differentiated into osteoblasts (Fig. 1l and n). Treatment with FGF2 and 200 μM SOS led to a dramatic increase in osteocalcin expression and complete closure of the coronal and sagittal sutures (Fig. 1o and p). Thus, these organ

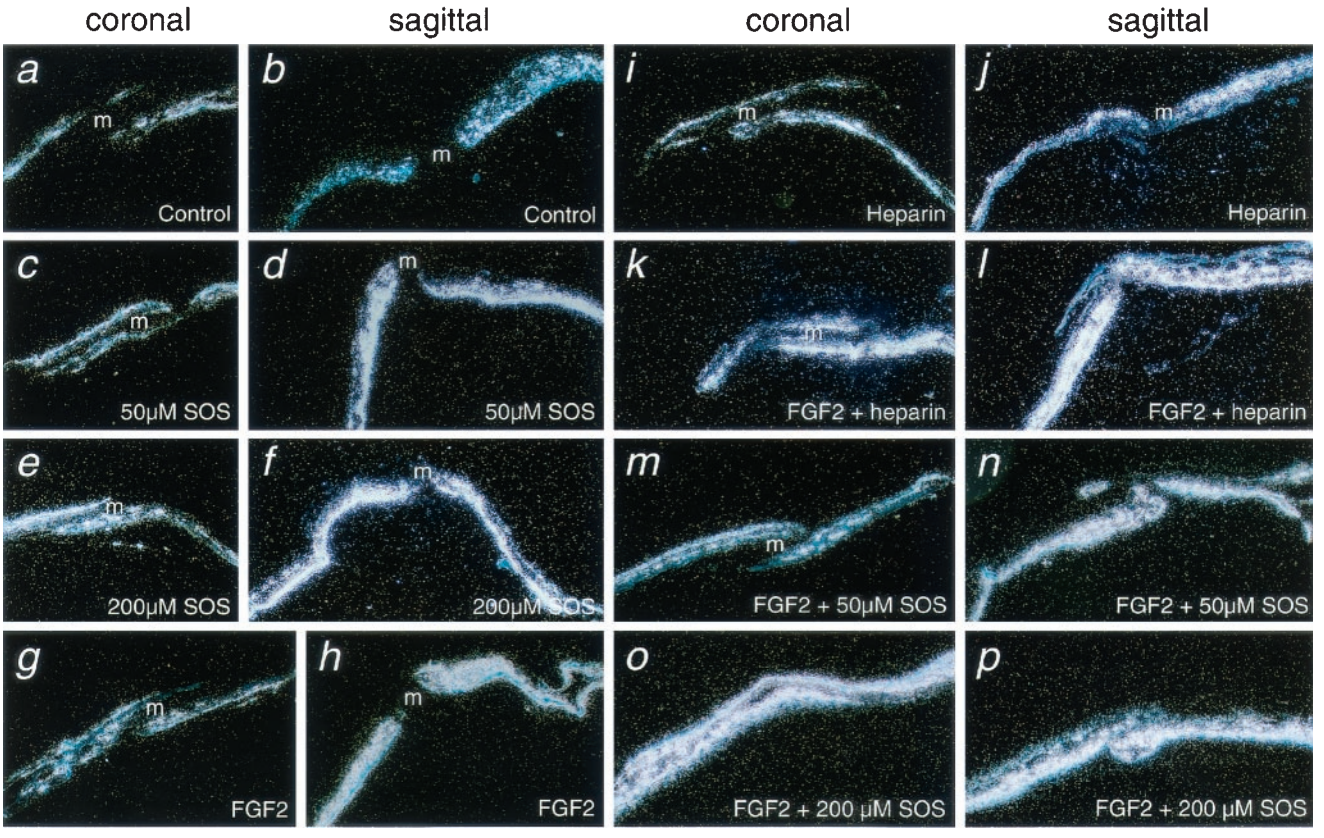


FIG. 1. Morphological changes and osteocalcin expression in 16.5-dpc mouse calvaria after culture in vitro in the presence or absence of FGF2, heparin, and SOS, alone or in combination. Frontal sections were taken at the coronal (a, c, e, g, i, k, m, and o) and sagittal (b, d, f, h, j, l, n, and p) sutures. Note the dramatic increase in osteocalcin expression in the presence of FGF2 and 200 μM SOS (o and p). m, mesenchyme.

culture data reaffirm the ability of SOS to imitate heparin action in stimulating FGF signaling.

**SOS can dimerize the FGF-FGFR complex.** Because activation of FGF signaling is strictly dependent on receptor dimerization, it was pertinent to check whether SOS is capable of dimerizing the FGF-FGFR complex. A 1:1 binary FGF2-FGFR1 complex was purified and mixed with SOS at various molar ratios. The resulting mixtures were analyzed by size exclusion chromatography. SOS induced dimerization of the FGF2-FGFR1 complex in a concentration-dependent manner (Fig. 2a to c). At a complex-SOS molar ratio of 1:1, we observed quantitative dimerization of the FGF2-FGFR1 complex (Fig. 2c).

To elucidate the structural mechanism by which SOS dimerizes FGF2-FGFR1 complexes, we crystallized the purified 2:2:2 FGF2-FGFR1-SOS dimer. Orthorhombic crystals containing two FGF2-FGFR1-SOS dimers in the asymmetric unit were obtained. Data collection and refinement statistics are given in Table 1.

**SOS dimerizes the FGF-FGFR complex in a manner reminiscent of the two-end model.** Each dimer exhibits a twofold symmetric assembly of two 1:1:1 FGF2-FGFR1-SOS ternary complexes reminiscent of the dimeric FGF2-FGFR1-heparin structure (Fig. 3a and c) (40). Within the dimer, each FGF binds to both FGFRs and the two FGFRs contact each other through their D2 portions. The C-terminal ends of the two receptors are predicted to insert into the plasma membrane at the membrane-proximal side of the dimer and are about 50 Å apart. This distance is similar the distance between the membrane insertion points of the ligand-induced erythropoietin receptor dimers (47). A deep canyon, the hallmark of the two-end model, is formed on the membrane-distal side of the dimer between the adjoining FGFR D2s and wanes as it reaches the ligands.

Two SOS molecules are observed to bind in this heparin-binding canyon (Fig. 3a). The $F_o$-$F_c$ electron density is strong and well defined for one of the two SOS molecules (Fig. 3b) and weaker for the other molecule. Nevertheless, the observed electron densities for both molecules are sufficiently strong to reveal that the two SOS molecules bind in a symmetric head-to-head fashion as the two heparin molecules do in the FGF2-FGFR1-heparin structure (40). This difference in electron density suggests that SOS binds tighter to one site than the other in the dimer. As with the dimeric FGF2-FGFR1 structure, the FGF2-FGFR1-SOS dimer exhibits a slight asymmetry in the orientation of the D2s (37). This asymmetry results in SOS binding tighter to one half of the heparin-binding canyon than to the other half.

Compared to heparin, SOS occupies mainly the deep portion of the heparin-binding canyon consisting of D2s of both FGFR1s and the FGF2 heparin-binding site adjacent to the receptors (Fig. 3a and c). This is in contrast to the crystal

TABLE 1. X-ray data collection and refinement statistics

| Parameter | Value |
|---|---|
| Data Collection | |
| Resolution (Å) | 30.0–2.6 |
| Observations | 764,014 |
| Unique reflections | 53,698 |
| Completeness[a] (%) | 99.9 (100.0) |
| $R_{sym}$[a,b] | 7.8 (33.2) |
| Refinement | |
| No. of atoms | |
| Protein | 10,823 |
| SOS | 220 |
| Water | 42 |
| $SO_4^{2-}$ | 15 |
| Resolution (Å) | 25.0–2.6 |
| Reflections | 52,014 |
| $R_{cryst}/R_{free}$[c] (%) | 24.1/27.8 |
| Root mean square deviations | |
| Bond lengths (Å) | 0.008 |
| Bond angles (°) | 1.4 |
| B factors[d] (Å$^2$) | 1.00 |
| Average B factors (Å$^2$) | |
| All atoms | 40.91 |
| Protein | 39.97 |
| SOS | 76.06 |

[a] The overall (30.0- to 2.6-Å) value is given first, with the value for the highest-resolution shell (2.69 to 2.6 Å) given in parentheses.
[b] $R_{sym} = 100 \times \Sigma|I - (I)|/\Sigma I$.
[c] $R_{cryst} = 100 \times \Sigma||F_O| - |F_c||/\Sigma|F_o|$, where $F_o$ and $F_c$ are the observed and calculated structure factors, respectively ($F_o > 0_\sigma$). $R_{free}$ was determined from 5% of the data.
[d] For bonded protein atoms.

structure of SOS bound to FGF only (50), where SOS binds to the FGF high-affinity heparin-binding site, which topologically corresponds to the distal shallow portion of the heparin-binding canyon. Moreover, opposite orientations of SOS, with respect to FGF, between the binary FGF-SOS and ternary FGF-FGFR-SOS structures are observed. Despite this disparity, the overall conformations of SOS for these two structures are similar.

Within each FGF2-FGFR1-SOS ternary complex, SOS makes four hydrogen bonds with FGFR1 and five hydrogen bonds with FGF2 (Fig. 4). As for heparin, concurrent binding of SOS to FGF and FGFR clearly promotes FGF-FGFR affinity. Interactions of SOS with FGFR1 involve Lys-163 and Lys-177, which protrude from the heparin-binding surface of D2, and the sulfate groups of both the five- and six-member rings of SOS (Fig. 4). These very same lysines bind heparin in the FGF2-FGFR1-heparin structure (40). At the SOS-FGF2 interface, a total of five hydrogen bonds between Lys-26 and Lys-135 of FGF2 and the sulfate groups of SOS are made (Fig. 4). Likewise, in the FGF2-FGFR1-heparin structure, these very same lysines also bind heparin (40). Compared to heparin, SOS makes five and nine fewer hydrogen bonds with FGFR1 and FGF2, respectively. Thus, the structure indicates that SOS enhances FGF2-FGFR1 affinity, albeit with lower efficacy than heparin.

Like heparin in the dimeric FGF2-FGFR1-heparin structure, SOS also interacts with D2 of the adjoining FGFR1 across the twofold axis. Five hydrogen bonds between SOS and D2 are made at this interface, just one less than at the corresponding interface in the FGF2-FGFR1-heparin structure.

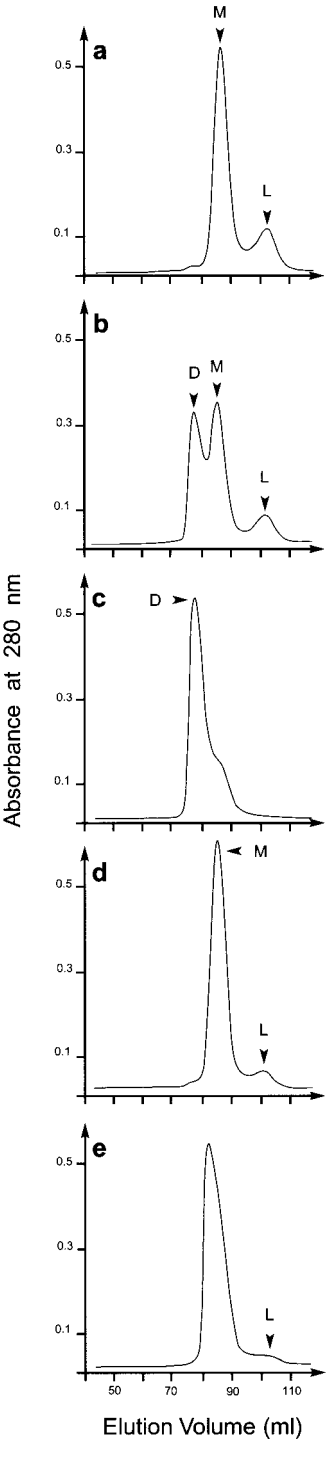


FIG. 2. SOS can dimerize an FGF2-FGFR1 complex. Aliquots of a purified 1:1 FGF2-FGFR1 complex (2 mg) were mixed at various molar ratios with SOS or selectively desulfated SOS analogs, and the reaction mixtures were analyzed by size exclusion chromatography. (a) Control (no SOS added); (b), 1:0.5 complex-SOS; (c) 1:1 complex-SOS; (d) 1:1 complex–4,6-dihydroxysucrose hexasulfate; (e) 1:1 complex–2-hydroxysucrose heptasulfate. M and D, elution positions of monomers and dimers, respectively; L, position of free FGF2 ligand, which results from the dissociation of FGF2-FGFR1 complexes due to protein dilution during size exclusion chromatography. Note that the addition of SOS reduces the free FGF2 peak as SOS increases FGF2-FGFR1 affinity.

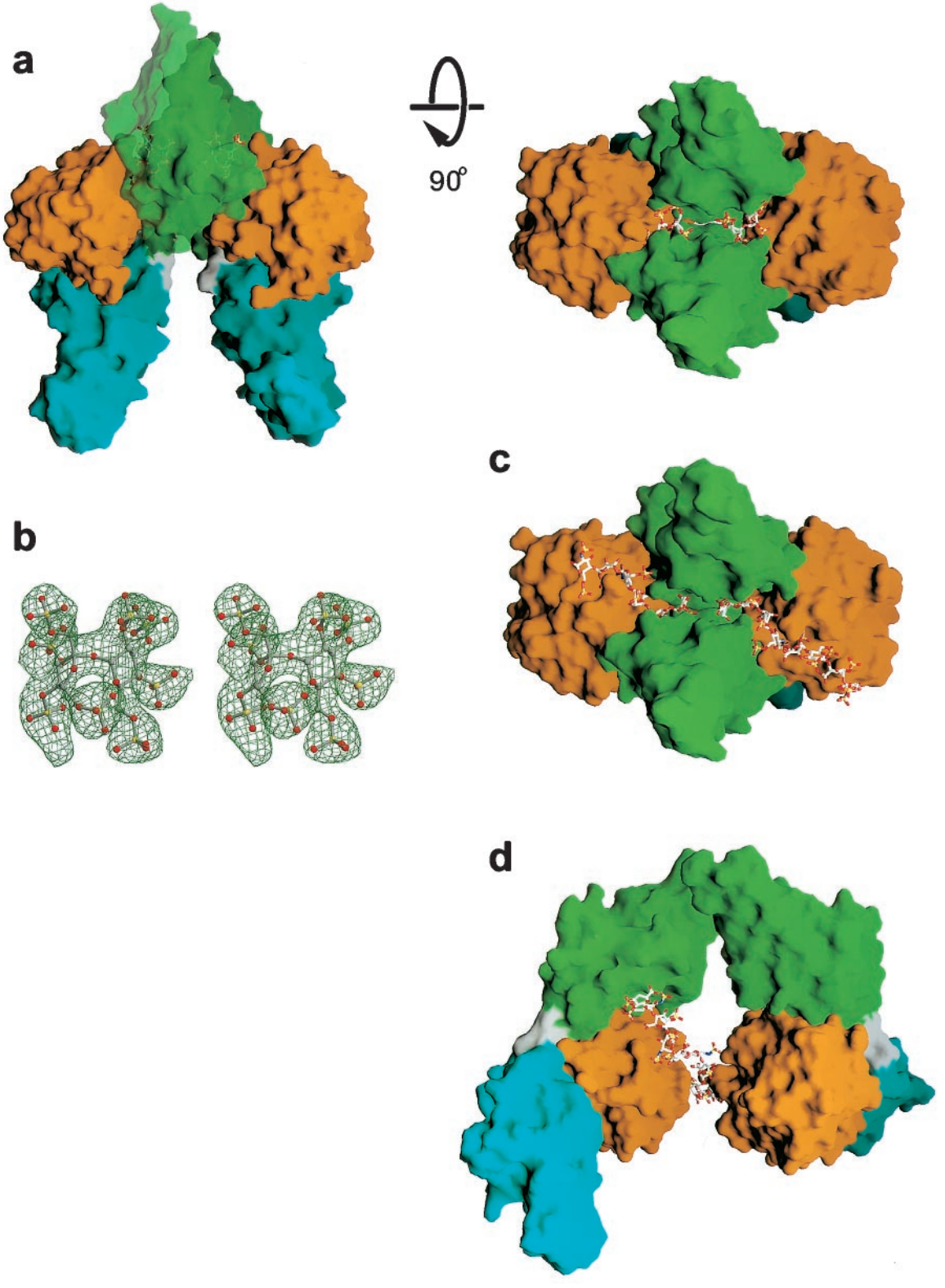


FIG. 3. Crystal structure of the FGF2-FGFR1-SOS complex. (a) Molecular surface representation of the 2:2:2 FGF2-FGFR1-SOS dimer in the asymmetric unit. Color coding is as follows: D2, green; D3, cyan; D2-D3 linker, gray; FGF2, orange. The D2 closer to the viewer is rendered partially transparent in the left view. SOS molecules are rendered in ball and stick. Atom coloring is as follows: red, oxygen; yellow, sulfur; blue, nitrogen; white-gray, carbon. The figure was made with GRASP (27). (b) Stereo view of the $F_o$-$F_c$ electron density map computed after simulated annealing with SOS omitted from the atomic model. The map is computed at 2.6-Å resolution and contoured at 2.6 σ. Atom coloring is as above. This figure was made with Bobscript (10). (c) Molecular surface representation of the 2:2:2 FGF2-FGFR1-heparin dimer (the symmetric two-end model) (40). (d) Molecular surface representation of the 2:2:1 FGF1-FGFR2-heparin dimer (the asymmetric alternative model) (33).

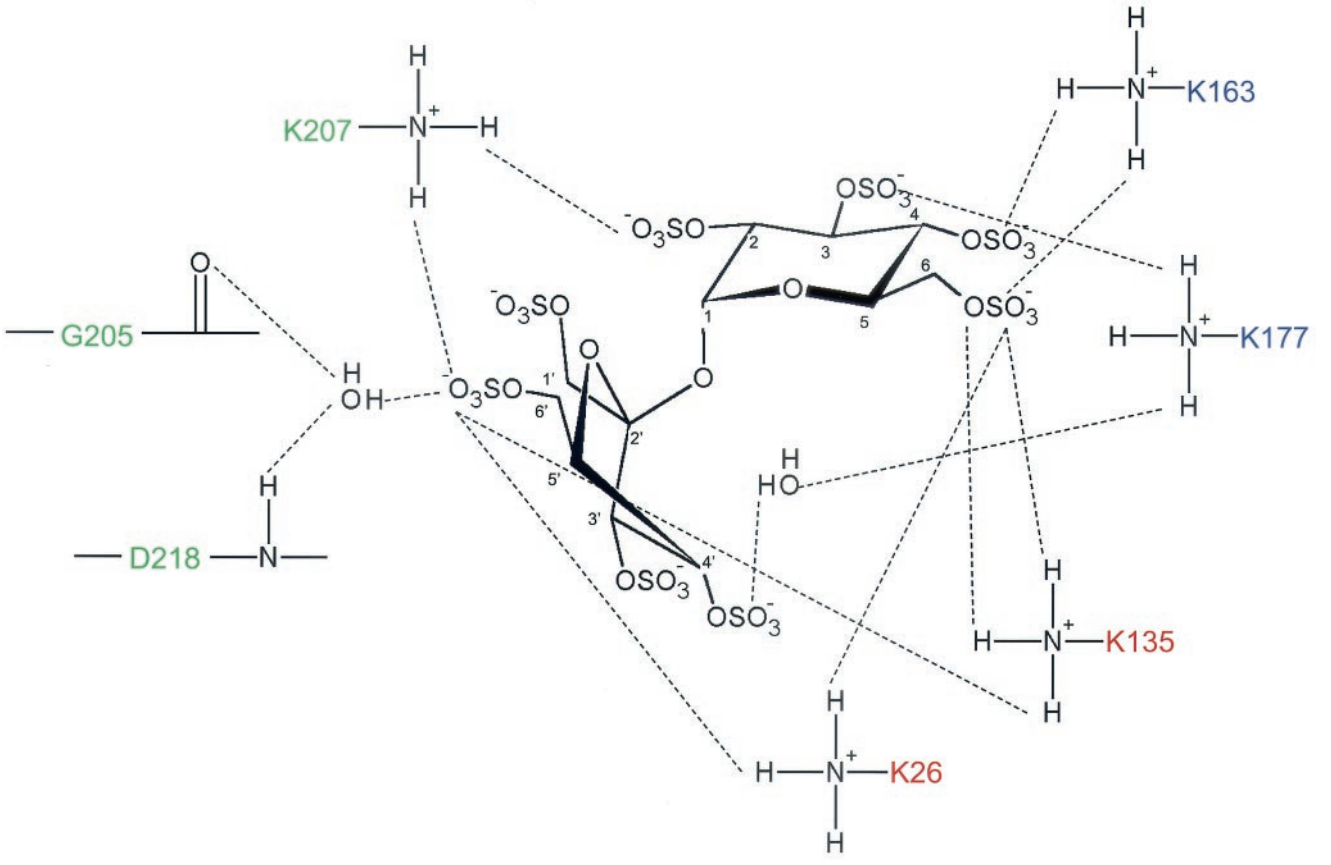


FIG. 4. Schematic diagram of the interactions between SOS, FGF2, and FGFR1. Dashed lines, hydrogen bonds. The backbone atoms of SOS are numbered according to International Union of Pure and Applied Chemistry nomenclature. The type and number of interacting residues are colored based on the molecule to which they belong. Coloring is as follows: FGF2, red, D2 of the primary FGFR1, blue; D2 of the adjoining FGFR1, green.

Lys-207 of FGFR1 D2 makes two hydrogen bonds with 2-sulfate (in the six-member ring) and 6′-sulfate (in the five-member ring) of SOS (Fig. 4). In addition, two water-mediated hydrogen bonds between the backbone atoms of FGFR1 D2 and the 6′-sulfate of SOS from the adjoining complex are made (Fig. 4). In the FGF2-FGFR1-heparin structure, Lys-207 is also implicated in heparin binding (40). These hydrogen bonds sustain the contacts between FGF and FGFR from one ternary complex with FGFR D2 in the adjoining ternary complex. Thus, the structure demonstrates that SOS also mimics heparin in promoting receptor dimerization.

To provide biochemical support for the observed mode of FGF-FGFR dimerization by SOS, we synthesized two SOS analogs lacking selected sulfate groups and tested these analogs for the ability to induce dimerization of FGF2-FGFR1 complexes in vitro (Fig. 2d and e). One analog, 4,6-dihydroxysucrose hexasulfate, was totally incapable of dimerizing the FGF2-FGFR1 complex (Fig. 2d). Since the 4 and 6 sulfates of SOS are involved in augmenting FGF2-FGFR1 affinity (Fig. 4), these data indicate that stabilization of the FGF-FGFR complex is a requisite for receptor dimerization. In the presence of the other analog, 2-hydroxysucrose heptasulfate, no peak corresponding to the FGF2-FGFR1-SOS dimer was observed as well (Fig. 2e). However, in this case the, FGF2-FGFR1 complex eluted slightly earlier than the control (Fig. 2a), indicating that the average Stokes radius of the FGF2-FGFR1 complex is slightly larger in the presence of the analog. This suggests that 2-hydroxysucrose heptasulfate may weakly dimerize the FGF2-FGFR1 complex. Indeed, according to the structure, the presence of the 6′-sulfate in this analog would allow this analog to minimally interact with adjoining FGFR and cause marginal receptor dimerization (Fig. 4). Taken together, the reduced abilities of the two SOS analogs to induce receptor dimerization confirm the structural mechanism by which SOS dimerizes the FGF-FGFR complex.

## DISCUSSION

Prior studies have shown that SOS can promote FGF signaling (2, 11, 29, 39, 45). In this report, we extend these studies by demonstrating that SOS, like heparin, evokes FGF-dependent differentiation in organ cultures. To provide a molecular basis for the heparin-like activity of SOS, we first demonstrated that SOS can dimerize FGF-FGFR complexes in vitro. We then determined the crystal structure of the dimeric FGF2-FGFR1-SOS complex. This structure reveals the symmetric association of two 1:1:1 FGF2-FGFR1-SOS ternary complexes reminiscent of the FGF2-FGFR1-heparin structure. Analysis

of the dimer unequivocally illustrates that SOS, merely a sulfated disaccharide, functionally imitates heparin by enhancing FGF-FGFR affinity and dimerization. Thus, we conclude that SOS promotes FGF signaling by promoting FGF-dependent FGFR activation.

Beyond providing a molecular basis for the heparin-like activity of SOS, the dimeric FGF2-FGFR1-SOS structure helps resolve the present uncertainty concerning the exact mode of FGFR dimerization. As introduced above, two competing models for FGFR dimerization by heparin and FGF have been proposed (Fig. 3c and d). Despite fundamental differences in their proposed mechanisms of receptor dimerization, both models have a common feature. In both models, one can readily identify a common ternary complex consisting of one FGF, one heparin, and D2 of one FGFR chain. Within this ternary complex, heparin interacts with FGFR through the terminal disaccharide unit at its nonreducing end and with FGF via the segment preceding the terminal disaccharide unit. Thus, both models convincingly corroborate, at the molecular level, the experimentally documented role of heparin in stabilizing the binary FGF-FGFR complex (31, 48).

The two models diverge when the predicted minimal heparin chain length capable of inducing FGF-FGFR dimerization is considered. In the two-end model a hexasaccharide is sufficient for promoting FGF-FGFR affinity and dimerization (40). Moreover, this model predicts that sugars as small as a disaccharide can have activity, as a disaccharide is still predicted to provide the minimal number of contacts with FGF and FGFR that are absolutely essential for increased ligand-receptor affinity and dimerization. In contrast, the total lack of protein-protein contacts between the two FGF-FGFR protomers in the Pellegrini model demands a heparin span of at least eight sugars for minimal receptor activation. This octasaccharide is predicted to cross-link the two ligands and to marginally engage one of the FGFR D2s (Fig. 3d) (33).

The dimeric FGF2-FGFR1-SOS structure is entirely consistent with and further reinforces the two-end dimerization model. Accumulating structural data demonstrate that FGF in the absence of heparin can form a low-affinity 1:1 complex with FGFR (17, 36, 37, 42). This complex has the potential to dimerize with another 1:1 binary complex through the concerted binding of FGF and FGFR from one complex to FGFR in another complex, albeit at high protein concentrations (37). However, at physiological concentrations these binary complexes tend to break up and thus fail to dimerize. According to the two-end model, the binding of heparin or SOS to binary FGF-FGFR complexes generates tight ternary complexes (FGF-FGFR-heparin or FGF-FGFR-SOS), which are less likely to dissociate than the binary FGF-FGFR complexes. These stabilized ternary complexes now have sufficient opportunity to dimerize through the concerted binding of FGF and FGFR from one ternary complex to FGFR from another ternary complex. Thus, a major role of heparin or SOS in FGF-FGFR dimerization is to generate stable FGF-FGFR complexes, which then provide sufficient interface for the binding of a second FGFR molecule. The inability of 4,6-dihydroxysucrose hexasulfate to dimerize the FGF2-FGFR1 complex is consistent with this hypothesis (Fig. 2d). In addition to enhancing FGF-FGFR affinity within the ternary complex, heparin and SOS interact with the heparin-binding sites in FGFR D2 of the adjoining ternary complex. These interactions further promote dimerization by fortifying the interactions of FGF and FGFR in one ternary complex with FGFR from the adjoining ternary complex.

It is difficult to reconcile the heparin-like activity of SOS with the Pellegrini model, where a heparin-linked FGF dimer is the sole driving force for receptor dimerization (33). SOS does not seem to dimerize FGFs in solution (2, 9, 41). Moreover, the FGF1-SOS crystal structure shows that only a single SOS molecule binds to the high-affinity heparin-binding site of FGF1 (50). Even if one were to assume that SOS dimerizes FGFs, it is not clear how a SOS sandwiched between two FGFs would be able to simultaneously engage the receptor as well.

In addition to SOS, other small polysulfonated molecules, including *myo*-inositol hexasulfate (MIHS) and sulfated β-cyclodextrin, have been reported to potentiate FGF actions (12, 25, 35). Like SOS, MIHS and β-cyclodextrin also bind to and stabilize FGFs (7, 35). Notably, MIHS and β-cyclodextrin also do not induce dimerization of FGFs (15, 25). Thus, it is unlikely that these molecules promote FGF signaling by dimerizing FGFs. We suggest that these molecules, like SOS and heparin, directly promote FGF-induced FGFR dimerization and activation.

Since a small sugar such as SOS can mimic heparin action, the criteria for the sulfation and length of heparin sufficient for FGFR dimerization need to be reevaluated. The smallest heparin molecule suggested to promote FGFR dimerization is a hexasaccharide (40). Although SOS is only two sugars long, its high sulfate content enables it to interact with the heparin-binding sites on FGF and FGFR in a manner sufficient for FGFR dimerization. Thus, high levels of sulfation can reduce the length requirement for supporting receptor dimerization and activation. This hypothesis is perhaps best supported by the ability of sulfated monosaccharide MIHS to induce FGF-dependent FGFR dimerization and activation (25, 35).

The structural data presented in this paper also afford a potential molecular mechanism for the ulcer-healing activity of sucralfate, the aluminum salt of SOS. Sucralfate is used to treat gastric and duodenal ulcers (43). Folkman et al. have shown that, unlike that of the conventional antiulcer drugs, the ulcer-healing activity of sucralfate does not involve adjustment of the stomach pH or antimicrobial activity (11). Instead, they showed that SOS is the active component of sucralfate and postulated that SOS heals ulcers by binding to and prolonging the half-lives of FGFs in the acidic milieu of the stomach, thereby promoting FGF-induced neoangiogenesis. In addition, our structural data imply that SOS exerts its ulcer-healing activity by promoting FGF-dependent FGFR dimerization and activation, which can occur in the vascular endothelium.

FGFs and FGFRs are also implicated in a variety of human skeletal disorders, including dwarfism and the craniosynostosis syndromes (24). In adult organisms, FGFs are thought to be involved in physiological angiogenesis and wound healing as well as in pathological angiogenesis, such as in tumor neovascularization and diabetic retinopathy (3, 13, 16). Consequently, the FGF2-FGFR1-SOS structure provides a template for the development of new therapeutic agents that modulate FGF signaling, particularly in light of limitations in the synthesis of homogeneously sulfated heparin oligosaccharides (34). Be-

cause the synthesis of homogeneously sulfated sucrose derivatives is straightforward, SOS derivatives are attractive candidates for novel therapeutics (4, 38, 44).

## ACKNOWLEDGMENTS

We thank Craig Ogata for synchrotron beamline assistance. Beamline X4A at the National Synchrotron Light Source, a Department of Energy facility, is supported by the Howard Hughes Medical Institute. We are grateful to Irma Thesleff for advice and inspiration in calvaria culture, to Tilmann Wurtz for the osteocalcin probe, and to Daniel Bar-Shalom and BM Research (Denmark) for providing SOS. We thank Omar Ibrahimi for critical reading of the manuscript.

This work was supported by grants from the National Institutes of Health (DE-13686 to M.M.; HL-62244 and HL-52622 to R.J.L.), the Swedish Medical Research Council (2789 and 14100 to A.G.L.), and the Jubileum Kliniken (to A.G.L.).

## REFERENCES

1. **Arakawa, T., J. Wen, and J. S. Philo.** 1993. Densimetric determination of equilibrium binding of sucrose octasulfate with basic fibroblast growth factor. J. Protein Chem. **12:**689–693.
2. **Arunkumar, A. I., T. K. Kumar, K. M. Kathir, S. Srisailam, H. M. Wang, P. S. Leena, Y. H. Chi, H. C. Chen, C. H. Wu, R. T. Wu, G. G. Chang, I. M. Chiu, and C. Yu.** 2002. Oligomerization of acidic fibroblast growth factor is not a prerequisite for its cell proliferation activity. Protein Sci. **11:**1050–1061.
3. **Battegay, E. J., M. Hagedorn, and A. Bikfalvi.** 1995. Angiogenesis: mechanistic insights, neovascular diseases, and therapeutic prospects. J. Mol. Med. **73:**333–346.
4. **Bazin, H. G., I. Capila, and R. J. Linhardt.** 1998. Conformational study of synthetic delta 4-uronate monosaccharides and glycosaminoglycan-derived disaccharides. Carbohydr. Res. **309:**135–144.
5. **Boudreaux, J. M., and D. A. Towler.** 1996. Synergistic induction of osteocalcin gene expression: identification of a bipartite element conferring fibroblast growth factor 2 and cyclic AMP responsiveness in the rat osteocalcin promoter. J. Biol. Chem. **271:**7508–7515.
6. **Brunger, A. T., P. D. Adams, G. M. Clore, W. L. DeLano, P. Gros, R. W. Grosse-Kunstleve, J. S. Jiang, J. Kuszewski, M. Nilges, N. S. Pannu, R. J. Read, L. M. Rice, T. Simonson, and G. L. Warren.** 1998. Crystallography and NMR system: a new software suite for macromolecular structure determination. Acta Crystallogr. D Biol. Crystallogr. **54:**905–921.
7. **Burke, C. J., D. B. Volkin, H. Mach, and C. R. Middaugh.** 1993. Effect of polyanions on the unfolding of acidic fibroblast growth factor. Biochemistry **32:**6419–6426.
8. **Chauvin, C., K. Baczko, and D. Plusquellec.** 1993. New highly regioselective reactions of unprotected sugars: synthesis of 2-*O*-acylsucrose and 2-*O*-(*N*-alkylcarbamoyl)sucrose. J. Org. Chem. **58:**2291–2295.
9. **DiGabriele, A. D., I. Lax, D. I. Chen, C. M. Svahn, M. Jaye, J. Schlessinger, and W. A. Hendrickson.** 1998. Structure of a heparin-linked biologically active dimer of fibroblast growth factor. Nature **393:**812–817.
10. **Esnouf, R. M.** 1997. An extensively modified version of MolScript that includes greatly enhanced coloring capabilities. J. Mol. Graph. Model. **15:**112–113 and 132–134.
11. **Folkman, J., S. Szabo, M. Stovroff, P. McNeil, W. Li, and Y. Shing.** 1991. Duodenal ulcer. Discovery of a new mechanism and development of angiogenic therapy that accelerates healing. Ann. Surg. **214:**414–425.
12. **Folkman, J., P. B. Weisz, M. M. Joullie, W. W. Li, and W. R. Ewing.** 1989. Control of angiogenesis with synthetic heparin substitutes. Science **243:**1490–1493.
13. **Friesel, R. E., and T. Maciag.** 1995. Molecular mechanisms of angiogenesis: fibroblast growth factor signal transduction. FASEB J. **9:**919–925.
14. **Gritli-Linde, A., P. Lewis, A. P. McMahon, and A. Linde.** 2001. The whereabouts of a morphogen: direct evidence for short- and graded long-range activity of hedgehog signaling peptides. Dev. Biol. **236:**364–386.
15. **Guzman-Casado, M., J. M. Sanchez-Ruiz, M. El Harrous, G. Gimenez-Gallego, A. Parody-Morreale, H. Zheng, P. K. Shah, and K. L. Audus.** 2000. Energetics of myo-inositol hexasulfate binding to human acidic fibroblast growth factor: effect of ionic strength and temperature. Eur. J. Biochem. **267:**3477–3486.
16. **Hagedorn, M., and A. Bikfalvi.** 2000. Target molecules for anti-angiogenic therapy: from basic research to clinical trials. Crit. Rev. Oncol. Hematology **34:**89–110.
17. **Ibrahimi, O. A., A. V. Eliseenkova, A. N. Plotnikov, K. Yu, D. M. Ornitz, and M. Mohammadi.** 2001. Structural basis for fibroblast growth factor receptor 2 activation in Apert syndrome. Proc. Natl. Acad. Sci. USA **98:**7182–7187.
18. **Johnson, D. E., L. T. Williams, A. Gritli-Linde, P. Lewis, A. P. McMahon, and A. Linde.** 1993. Structural and functional diversity in the FGF receptor multigene family. Adv. Cancer Res. **60:**1–41.
19. **Jones, T. A., J. Y. Zou, S. W. Cowan, and M. Kjeldgaard.** 1991. Improved methods for binding protein models in electron density maps and the location of errors in these models. Acta Crystallogr. A **47:**110–119.
20. **Khan, R., K. S. Mufti, and M. R. Jenner.** 1978. Synthesis and reactions of 4,5 acetals of sucrose. Carbohydr. Res. **65:**109–113.
21. **Kim, H. J., D. P. Rice, P. J. Kettunen, and I. Thesleff.** 1998. FGF-, BMP- and Shh-mediated signalling pathways in the regulation of cranial suture morphogenesis and calvarial bone development. Development **125:**1241–1251.
22. **Kleywegt, G. J., and T. A. Jones.** 1998. Databases in protein crystallography. Acta Crystallogr. D Biol. Crystallogr. **54:**1119–1131.
23. **Loughman, M. S., K. Chatzistefanou, E. M. Gonzalez, E. Flynn, A. P. Adamis, Y. Shing, R. J. D'Amato, and J. Folkman.** 1996. Experimental corneal neovascularisation using sucralfate and basic fibroblast growth factor. Aust. N. Z. J. Ophthalmol. **24:**289–295.
24. **McIntosh, I., G. A. Bellus, and E. W. Jab.** 2000. The pleiotropic effects of fibroblast growth factor receptors in mammalian development. Cell Struct. Funct. **25:**85–96.
25. **Middaugh, C. R., H. Mach, C. J. Burke, D. B. Volkin, J. M. Dabora, P. K. Tsai, M. W. Bruner, J. A. Ryan, and K. E. Marfia.** 1992. Nature of the interaction of growth factors with suramin. Biochemistry **31:**9016–9024.
26. **Navaza, J.** 1994. AMoRe: an automated package for molecular replacement. Acta Crystallogr. A **50:**157–163.
27. **Nicholls, A., K. A. Sharp, and B. Honig.** 1991. Protein folding and association: insights from the interfacial and thermodynamic properties of hydrocarbons. Proteins **11:**281–296.
28. **Ornitz, D. M.** 2000. FGFs, heparan sulfate and FGFRs: complex interactions essential for development. Bioessays **22:**108–112.
29. **Ornitz, D. M., A. B. Herr, M. Nilsson, J. Westman, C. M. Svahn, and G. Waksman.** 1995. FGF binding and FGF receptor activation by synthetic heparan-derived di- and trisaccharides. Science **268:**432–436.
30. **Ornitz, D. M., and N. Itoh.** 2001. Fibroblast growth factors. Genome Biol. **2:**1–12.
31. **Ornitz, D. M., A. Yayon, J. G. Flanagan, C. M. Svahn, E. Levi, and P. Leder.** 1992. Heparin is required for cell-free binding of basic fibroblast growth factor to a soluble receptor and for mitogenesis in whole cells. Mol. Cell. Biol. **12:**240–247.
32. **Otwinowski, Z., and W. Minor.** 1997. Processing of X-ray diffraction data collected in oscillation mode. Methods Enzymol. **276:**307–326.
33. **Pellegrini, L., D. F. Burke, F. von Delft, B. Mulloy, and T. L. Blundell.** 2000. Crystal structure of fibroblast growth factor receptor ectodomain bound to ligand and heparin. Nature **407:**1029–1034.
34. **Pervin, A., C. Gallo, K. A. Jandik, X. J. Han, and R. J. Linhardt.** 1995. Preparation and structural characterization of large heparin-derived oligosaccharides. Glycobiology **5:**83–95.
35. **Pineda-Lucena, A., M. A. Jimenez, J. L. Nieto, J. Santoro, M. Rico, and G. Gimenez-Gallego.** 1994. $^{1}$H-NMR assignment and solution structure of human acidic fibroblast growth factor activated by inositol hexasulfate. J. Mol. Biol. **242:**81–98.
36. **Plotnikov, A. N., S. R. Hubbard, J. Schlessinger, and M. Mohammadi.** 2000. Crystal structures of two FGF-FGFR complexes reveal the determinants of ligand-receptor specificity. Cell **101:**413–424.
37. **Plotnikov, A. N., J. Schlessinger, S. R. Hubbard, and M. Mohammadi.** 1999. Structural basis for FGF receptor dimerization and activation. Cell **98:**641–650.
38. **Polat, T., H. G. Bazin, and R. J. Linhardt.** 1997. Enzyme catalyzed regioselective synthesis of sucrose fatty acid ester surfactants. J. Carbohydr. Chem. **16:**1319–1325.
39. **Rashid, M. A., S. Akita, M. S. Razzaque, H. Yoshimoto, H. Ishihara, T. Fujii, K. Tanaka, and T. Taguchi.** 1999. Coadministration of basic fibroblast growth factor and sucrose octasulfate (sucralfate) facilitates the rat dorsal flap survival and viability. Plast. Reconstr. Surg. **103:**941–948.
40. **Schlessinger, J., A. N. Plotnikov, O. A. Ibrahimi, A. V. Eliseenkova, B. K. Yeh, A. Yayon, R. J. Linhardt, and M. Mohammadi.** 2000. Crystal structure of a ternary FGF-FGFR-heparin complex reveals a dual role for heparin in FGFR binding and dimerization. Mol. Cell **6:**743–750.
41. **Spivak-Kroizman, T., M. A. Lemmon, I. Dikic, J. E. Ladbury, D. Pinchasi, J. Huang, M. Jaye, G. Crumley, J. Schlessinger, and I. Lax.** 1994. Heparin-induced oligomerization of FGF molecules is responsible for FGF receptor dimerization, activation, and cell proliferation. Cell **79:**1015–1024.
42. **Stauber, D. J., A. D. DiGabriele, and W. A. Hendrickson.** 2000. Structural interactions of fibroblast growth factor receptor with its ligands. Proc. Natl. Acad. Sci. USA **97:**49–54.
43. **Szabo, S., D. Hollander, M. Hagedorn, and A. Bikfalvi.** 1989. Pathways of gastrointestinal protection and repair: mechanisms of action of sucralfate. Am. J. Med. **86:**23–31.
44. **Vlahov, I. R., P. I. Vlahova, and R. J. Linhardt.** 1997. Regioselective synthesis of sucrose monoesters as surfactants. J. Carbohydr. Chem. **16:**1–10.
45. **Volkin, D. B., A. M. Verticelli, K. E. Marfia, C. J. Burke, H. Mach, and C. R. Middaugh.** 1993. Sucralfate and soluble sucrose octasulfate bind and stabilize acidic fibroblast growth factor. Biochim. Biophys. Acta **1203:**18–26.

46. **Wilkinson, D. G., J. A. Bailes, J. E. Champion, and A. P. McMahon.** 1987. A molecular analysis of mouse development from 8 to 10 days post coitum detects changes only in embryonic globin expression. Development **99:**493–500.
47. **Wilson, I. A., and L. K. Jolliffe.** 1999. The structure, organization, activation and plasticity of the erythropoietin receptor. Curr. Opin. Struct. Biol. **9:**696–704.
48. **Yayon, A., M. Klagsbrun, J. D. Esko, P. Leder, and D. M. Ornitz.** 1991. Cell surface, heparin-like molecules are required for binding of basic fibroblast growth factor to its high affinity receptor. Cell **64:**841–848.
49. **Zheng, H., P. K. Shah, and K. L. Audus.** 1994. Primary culture of rat gastric epithelial cells as an in vitro model to evaluate antiulcer agents. Pharm. Res. **11:**77–82.
50. **Zhu, X., B. T. Hsu, and D. C. Rees.** 1993. Structural studies of the binding of the anti-ulcer drug sucrose octasulfate to acidic fibroblast growth factor. Structure **1:**27–34.